Relationship between Cloud Radiative Forcing and Sea Surface Temperatures over the Entire Tropical Oceans

M. H. ZHANG, R. D. CESS, AND S. C. XIE

Institute for Terrestrial and Planetary Atmospheres, State University of New York at Stony Brook, Stony Brook, New York

(Manuscript received 23 May 1995, in final form 27 November 1995)

ABSTRACT

Satellite measurements from January 1985 to December 1989 show that warmer tropical oceans as a whole are associated with less longwave greenhouse effect of clouds and less cloud reflection of solar radiation to the space. The regression slopes of longwave and shortwave cloud radiative forcings against sea surface temperatures averaged from 30°N to 30°S are about -3 and 2 W m^{-2} K^{-1}, respectively. Relationships of cloud forcings and sea surface temperatures are analyzed for regions with different sizes. As has been reported in previous studies, the magnitude of area-averaged cloud radiative forcing for both longwave and shortwave radiations increases with sea surface temperatures in the equatorial eastern Pacific and is insensitive to sea surface temperatures over the tropical Pacific basin. Yet, when the region extends beyond the tropical Pacific, the magnitude decreases with sea surface temperatures. This phenomenon is shown to relate to changes in clouds over the tropical Indian Ocean and Atlantic, where sea surface temperatures increased but clouds decreased during the 1987 El Niño event. Relevance of the results to other climate changes is discussed.

1. Introduction

Cloud–climate interactions constitute an area of significant uncertainty in projecting future climate change caused by anthropogenic activities (e.g., IPCC 1990). For example, variation of clouds associated with a CO_2-induced climate change can either amplify or mediate the direct radiative forcing of the increased CO_2 concentrations (Wetherald and Manabe 1988; Mitchell et al. 1989). One comparison of 19 general circulation models revealed drastic differences in one measure of the cloud feedbacks (Cess et al. 1990). A recent updated comparison by Cess et al. (1996) showed that disagreement in the net cloud feedback among the models has been reduced in the last several years, but there are still large disagreements in the longwave and shortwave components of cloud feedbacks. Since clouds are sensitive to model parameterizations, it is necessary to compare model results with observational data to improve our confidence in the models.

The present study analyzes the relationship between variations of cloud forcing and SSTs in the observational data. The purpose is twofold. The first is to show how the geographical compensatory variations of clouds determine the overall cloud effect over a global domain. The second purpose is to provide a special case of observed cloud–climate interaction for comparison with general circulation models. Many previous studies have examined the relationships of clouds and sea surface temperatures (e.g., Ramanathan and Collins 1991; Fu et al. 1992; Hartmann and Michelsen 1993; Arking and Ziskin 1994). These studies fall into two categories. One deals with the clouds–SST relationship on regional scales, particularly in areas where clouds are strongly coupled with SSTs (Ramanathan and Collins 1991). The other deals with relationships of clouds and SSTs averaged over a large domain (Fu et al. 1992; Hartmann and Michelsen 1993; Chou 1994). This second type of study does not directly address the regional regulation of clouds to maximum SSTs or to the SST gradient. Yet, such studies are relevant for addressing the overall impact of clouds on the radiation budget. These studies take into account the compensatory changes of clouds over different regions. Ideally, the size of the domain should encompass the whole globe. But practically, if the domain is too large, variations of the averaged SST could be small, and the signature of the SST variations and cloud effects could be indistinguishable from noises.

The present investigation belongs to the second category of studies dealing with cloud–SST relationships. We report an important phenomenon during the period from 1985 to 1989—namely, that the magnitude of longwave cloud forcing, averaged over the whole of the Tropics from 30°N to 30°S, decreases with SST, a cooling effect with a rate of about -3 W m^{-2} K^{-1}. This

Corresponding author address: Dr. Minghua Zhang, Institute for Terrestrial and Planetary Atmosphere, State University of New York at Stony Brook, Stony Brook, NY 11794-5000.
E-mail: mzhang@atmsci.msrc.sunysb.edu

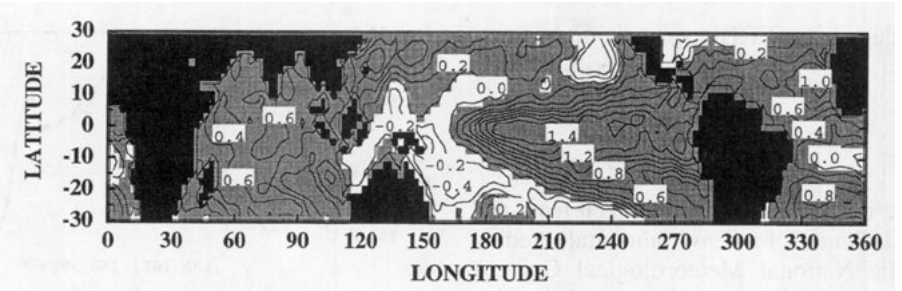

FIG. 1. Difference of sea surface temperatures (in K) between two 18-month means (January 1987–June 1988 minus January 1985–June 1986). Contour interval is 0.2. Positive area is shaded.

reduction of the greenhouse effect of clouds with SST is accompanied by a reduction in the cloud reflection of solar radiation, a warming effect, at a rate of about 2 W m^{-2} K^{-1}. The net effect after a large compensation between the longwave and shortwave cloud effects follows that of the longwave—a cooling effect. We present an analysis of the cloud radiative forcing (CRF)–SST relationships for regions with different sizes. We show that the CRF–SST relationship for the whole of the Tropics is opposite to that in the equatorial eastern Pacific, and the CRF–SST relationship for the tropical Pacific from 30°N to 30°S is in the middle, which is not statistically significant. We also show that this phenomenon is caused by changes of clouds over the tropical Indian Ocean and the Atlantic. This result complements previous studies in this category, which have reported that the basin-scale-averaged cloud forcing in the tropical Pacific is insensitive to SST variations.

The paper is organized in the following manner. Section 2 describes the data and procedure that were used. Section 3 presents the main results of the paper. A comparison is given between the clouds–SST relationships in different geographical domains. Also examined is the cause of the change of cloud forcing with SST. Section 4 discusses the relevance of the current results to other climate changes. The last section is a summary.

2. Data and procedure

a. Cloud radiative forcing

The data employed in this study are longwave and shortwave radiative fluxes at the top of the atmosphere (TOA) from the Earth Radiation Budget Experiments (ERBE). We used the combined S-4 product of *Earth Radiation Budget Satellite, NOAA-9,* and *NOAA-10* measurements, which is released from the National Aeronautic and Space Administration's Langley Research Center. The data include fluxes under both all-sky and clear-sky conditions gridded at a 2.5° lat × 2.5° long resolution. The implementation of ERBE, including the technique to separately measure all-sky and clear-sky fluxes, can be found in Barkstrom and Smith (1986), Ramanathan et al. (1989), and Harrison et al. (1990).

Cloud-radiative forcing is defined as the influence of clouds on the input of radiative energy to the earth–atmosphere system at the TOA. Its variation represents the feedback of clouds on the climate system. If we use F to denote the outgoing longwave radiation at the TOA and Q to denote the net downward shortwave radiation at the TOA, and if we use subscript c to denote clear-sky quantities, the longwave (LW) CRF is defined as

$$\text{LW CRF} = F_c - F. \tag{1}$$

It is typically positive, and it describes the reduction of longwave emission due to the presence of clouds (Ramanathan et al. 1989). The shortwave (SW) CRF is defined as

$$\text{SW CRF} = Q - Q_c. \tag{2}$$

It is typically negative. The net CRF, or the total CRF, is simply the sum of the two.

In deriving the CRF from ERBE, we face the problem of handling grids with missing clear-sky fluxes. In the ERBE S-4 product, if the instruments do not have a certain number of clear-sky pixel measurements in a month, then the 2.5° lat × 2.5° long grid box is considered to be missing for clear-sky fluxes. Although these grid boxes represent only a small percentage of the total grid boxes, they are in very cloudy regions, so that the magnitudes of CRFs are large. Several studies have discussed the impact of missing clear-sky fluxes on the evaluation of CRFs (Cess et al. 1992; Potter et al. 1992; Zhang et al. 1994). We have chosen in this study to fill the missing grid boxes with CRF values of maximum magnitude among the adjacent four boxes. Since we study cloud forcing over oceans that are relatively uniform on small scales, errors resulting from the filling are expected to be small. A sensitivity test is performed to first fill the missing clear-sky fluxes with values at the nearest grid boxes and then to calculate the CRFs at these grid boxes. The difference is found to be negligible.

The monthly data from ERBE span from January 1985 to December 1989. This 60-month period covers an El Niño event in 1987.

b. SST

The sea surface temperature data are taken from the monthly National Centers for Environmental Prediction (formerly the National Meteorological Center) analysis, which is derived from ship, buoy, and satellite measurements. The data are collocated in time and space with the TOA cloud radiative forcing from ERBE. Detailed description of the SST data can be found in Reynolds (1988).

Figure 1 shows the variation of SSTs between two parallel 18-month periods, January 1985 to June 1986 and January 1987 to June 1988 (the second period minus the first period). Associated with the 1987 El Niño event, SSTs in the central and eastern Pacific are more than 1 K warmer in the second period. Cooling occurs in the western Pacific, but the magnitude is less than 0.4 K. A notable feature is that in the tropical Indian Ocean and in the Atlantic, SSTs are also warmer in the El Niño period. The magnitude is as large as 0.6 K. This warming of the Indian Ocean and the Atlantic has been known to exist in other El Niño events as well (e.g., Trenberth and Shea 1987; Philander 1990).

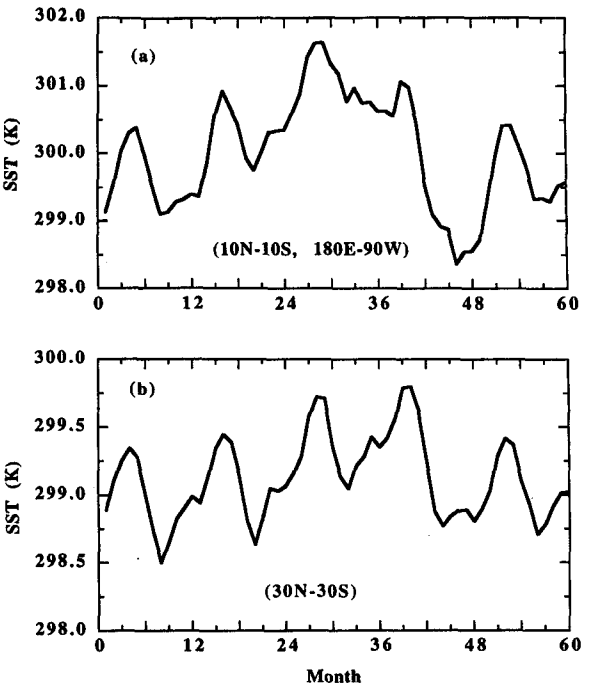

FIG. 2. Time variation of monthly mean SSTs starting from January 1985 for (a) the equatorial eastern Pacific and (b) the tropical oceans as a whole.

c. Seasonal versus interannual variations

Figure 2 shows the time variation of the averaged SST over the equatorial eastern Pacific (10°N–10°S, 180°E–90°W) and over the entire tropical oceans (30°N to 30°S). There are strong signals of seasonal variation in both regions. To examine the CRF–SST relationship, one would try to exclude external factors that could affect the variations of CRFs and SSTs. Since the seasonal variation is forced by variation of incoming solar radiation and lateral boundaries at higher latitudes, it is hardly possible that clouds are not affected by these influences. As a consequence, directly correlating clouds with SST may provide no information about how clouds respond to SST change in the present circumstances, where clouds and SSTs may not be strongly coupled.

We therefore filter out the seasonal components of cloud and SST variations. This is done by subtracting the monthly climatology from each month of the data. The 12-month climatology is constructed by using the average of the 5-yr data. We understand that the period is short for defining an accurate climate annual component. However, this is the total duration of the ERBE instruments with narrow field-of-view measurements. We caution that the results presented in the following section are applicable to this particular period of time; further discussion is presented in section 4 about their relevance to other time periods.

The interannual variability of CRFs and SSTs for 60 months constitutes the main dataset in our analysis. In the following, relationships between clouds and SSTs are also examined on longer timescales; these are analyzed, of course, at the expense of reducing the number of time samples. Interannual variability of collocated cloud amount from the International Satellite Cloud Climatology Project and atmospheric circulations from the European Centre for Medium-Range Weather Forecasts analysis are also used.

3. Results

Since our purpose is to take into account compensatory changes of clouds and SSTs in different parts of the world, we use area-averaged quantities to examine the CRF–SST relationships. Various spatial domains are used in an attempt to examine where and how significant these compensatory changes are, and whether clouds and SSTs are coupled locally. It should be pointed out that if clouds in the whole of the Tropics respond only to SST variations in the equatorial Pacific, averaging SSTs over the whole of the Tropics may underestimate the SST signature. On the other hand, if SSTs in the tropical Pacific can affect clouds and SSTs in other parts of the Tropics, it is then appropriate to perform the averaging of SSTs over the whole of the Tropics.

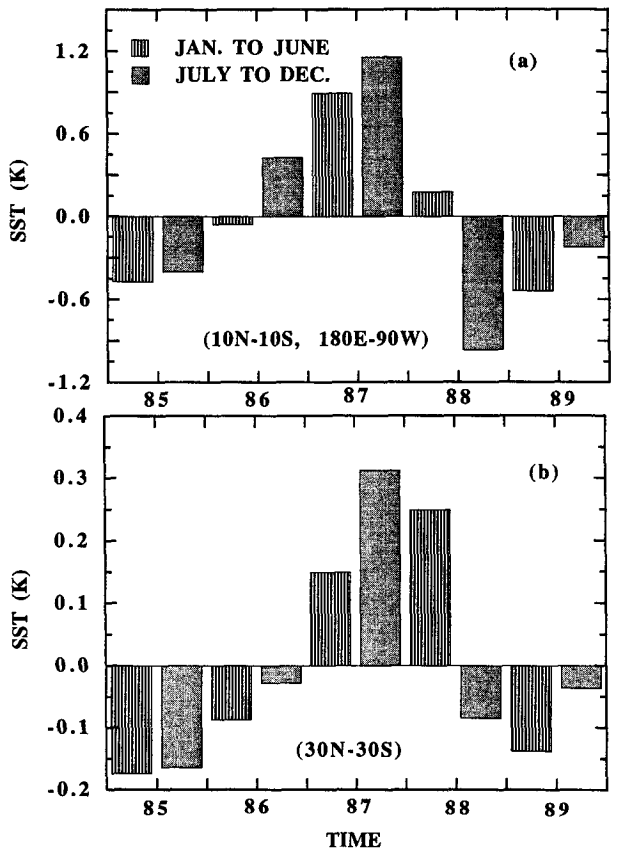

FIG. 3. Interannual variability of SSTs averaged to 6-month means for (a) the equatorial eastern Pacific and (b) the tropical oceans as a whole.

a. Regional versus global relations

Figure 3 shows the interannual variability of SST averaged in the equatorial eastern Pacific and over the tropical oceans as a whole (from 30°N to 30°S). Plotted are 6-month averages. Corresponding to the 1987 El Niño, SST anomalies in the equatorial eastern Pacific are positive from the later half of 1986 to the beginning of 1988. The maximum reached more than 1 K, which is consistent with Fig. 1. For the entire Tropics, the positive anomaly reached 0.3 K in the second half of 1987. This anomaly is contributed to in part by the anomaly in the equatorial eastern Pacific shown in Fig. 3a. When we partition it into contributions from the equatorial eastern Pacific and from the rest of tropical oceans (by taking the anomaly in a particular region and weighing the area of this region against the area of the whole tropical oceans), the two parts are of equivalent magnitude. Contribution from areas beyond the equatorial eastern Pacific has been partly offset by cooling in the western Pacific.

To maximize the signal of cloud variations, we first take the two periods of January 1985–June 1986 and January 1987–June 1988, each of which has three consecutive 6-month averages. Figures 4a–c show the variation of CRFs in the equatorial eastern Pacific plotted against the SST anomalies. It is generally known that high SSTs in the Tropics correspond to more convection and larger magnitudes of cloud forcing. These are also shown in the figures as larger LW CRFs and smaller SW CRFs when SSTs are higher. We note that the LW CRF varies more with SST than does the SW CRF.

A very different relationship is found for the tropical oceans as a whole (Figs. 4d–f). Figure 4d shows that the averaged LW CRF decreases with the averaged SST, and the rate of change is significant. Thus, when the SST is warmer, there is less cloud trapping of longwave radiation—a cooling effect. As a result, for the SSTs, TOA longwave emission is enhanced, not only because of the increased temperature of the system, but also because of the reduction of longwave cloud forcing. We note that if all of the ten 6-month anomalies from 1985 to 1989 are used, the results remain the same, except that relatively more scatters appear in Fig. 4 associated with relatively small SST anomalies in other 6-month periods (see Fig. 3b).

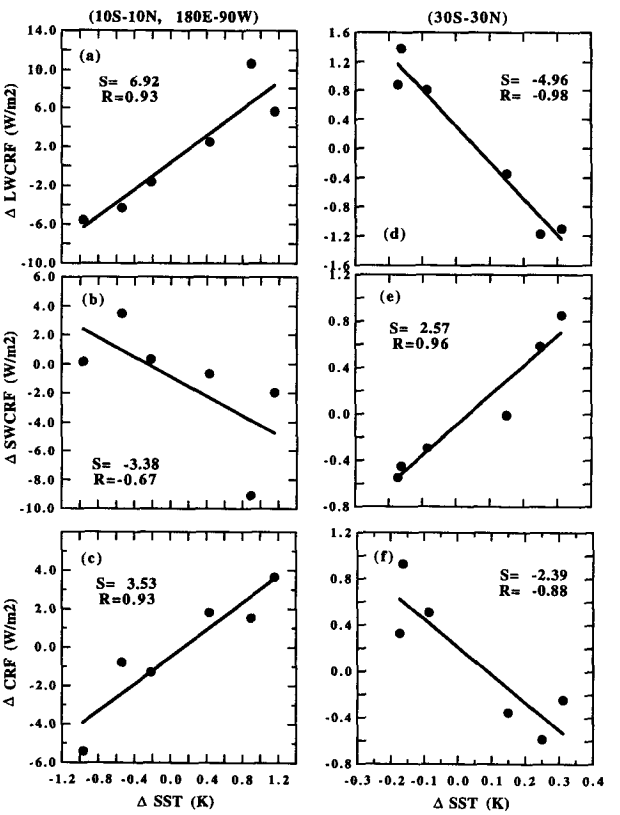

FIG. 4. Relationships of cloud-radiative forcings with SSTs for the two periods of January 1985–June 1986 and January 1987 to June 1988 using 6-month means: (a)–(c) are for the equatorial eastern Pacific and (d)–(e) are for tropical oceans as a whole.

To amplify this point, Fig. 5a gives the annual mean upward blackbody longwave emission at the ocean surface, averaged from 30°N to 30°S. Warm SSTs correspond to more emission. Figure 5b shows the TOA emission. Since the ordinate scales are the same in Figs. 5a and 5b, by looking at the flux change between 1985 and 1987, it is seen that the increase of TOA longwave emission in Fig. 5b is greater than that implied by the Stephen–Boltzman law when it is applied to the SSTs in Fig. 5a. From this figure alone, one can also argue that the enhanced emission may come from variation of the clear-sky greenhouse effect associated with water vapor. Indeed, Chou (1994) reported that the atmospheric clear-sky greenhouse effect in the tropical Pacific decreased from April 1985 to April 1987. We use Fig. 5c to show that the clear-sky greenhouse effect over tropical oceans as a whole is generally larger in a warmer year, so that more longwave radiation is trapped by the clear-sky atmosphere. Here, clear-sky greenhouse effect is defined as the difference between surface upward emission and the clear-sky TOA emission. Figure 5d shows the total-sky greenhouse effect, which reduced from 1985 to 1987. Figure 5e shows that it is the decrease of longwave cloud radiative forcing that contributes to the reduction of total greenhouse effect and makes the variation of TOA emission from 1985 to 1987 greater than that at the surface. Here, we reiterate that this analysis is applicable for the particular period of 1985 to 1989, during which an El Niño event occurred in 1987, and during which ERBE cloud forcing measurements were taken.

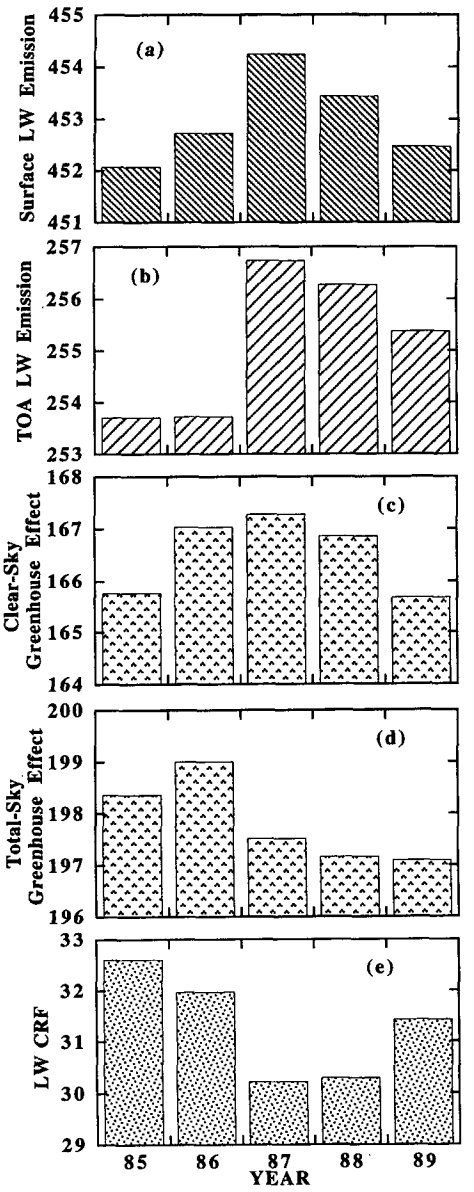

FIG. 5. Variation of annual mean radiative fluxes over the entire tropical oceans from 30°N to 30°S (in W m^{-2}). (a) Upward longwave emission at the surface. (b) Upward longwave emission at the TOA. (c) The atmospheric clear-sky greenhouse effect. (d) Atmospheric total-sky greenhouse effect. (e) Longwave cloud radiative forcing.

Naturally, variation of clouds also affects the shortwave radiation budget. Figure 4e shows that shortwave cloud forcing increases with SST. Since SW CRF is negative, producing a cooling effect on the earth–atmosphere system, an increase means a reduction in the reflective power of clouds as the SSTs warm up, a positive feedback. This is consistent with what can be expected from a change in the cloud amount. Reductions in clouds cause more TOA longwave emission (a cooling effect), and less reflection (a warming effect). We should caution that opposite changes in the longwave and shortwave CRFs cannot be taken for granted because of the intricate nature in the variations of cloud height, type, and cloud optical properties. Some general circulation models have produced changes of longwave and shortwave CRFs that have the same signs (Cess et al. 1991; Randall et al. 1992).

There is a large cancellation between variations of the longwave and shortwave cloud forcings. However, the LW CRF varies more than the SW CRF. As a result, the net cloud forcing decreases with SST, which means a net loss of radiation due to variations of clouds as SSTs become higher (Fig. 4f).

b. Domain dependence

The above discussion illustrates that the CRF–SST relationship over tropical oceans as a whole not only differs from the regional relationships reported in previous studies, but also differs from studies employing spatial averages in the Pacific basin. The dependence of the relationship on the size of the domain has been emphasized in Hartmann and Michelsen (1993). To study the cause of this dependence, and in particular, the sign reversal in the relationships, we employed the

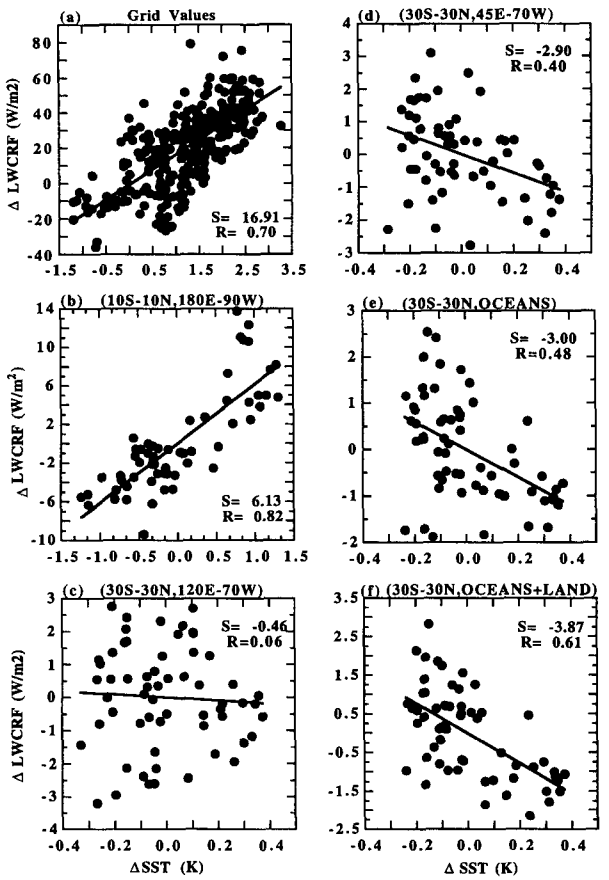

FIG. 6. Relationships between area-averaged LW CRF and SSTs in different regions obtained by employing 60-month mean data. Grid values are taken from the 2.5° lat × 2.5° long ERBE monthly data in the two months of April 1985 and April 1987 from 10°N to 10°S, 140°E to 90°W.

60-month data for different regions (Fig. 6). For comparison with other studies, we also include Fig. 6a, which shows the variation of LW CRF against SSTs at each grid box of 2.5° × 2.5° from April 1985 to April 1987 in the region of 10°N–10°S, 140°E–90°W. Figures 6b–f show the regression of area-averaged LW CRF against area-averaged SSTs for an expanding series of regions, starting from the equatorial eastern Pacific. It is seen that there is virtually no correlation between the cloud forcing and SSTs as far as the entire tropical Pacific is concerned (Fig. 6c). Yet, as the domain is extended to include the Indian Ocean, the relationship starts to reverse (Fig. 6d).

A minor point to be drawn from Fig. 6 is that there are scatters around any regression line, even when the correlation is high between the SSTs and CRF. Since one may obtain any CRF–SST relationship by just taking two specified months of data, a sufficient number of time samples is necessary for establishing a meaningful relationship.

A similar picture can be plotted for the SW CRF. The general features are the same, but the signs of the slopes are opposite those of the LW CRF because the two tend to compensate for each other. In Fig. 7, we present the regression ratios of the LW, SW, and total CRFs against SSTs obtained by employing all the 60-monthly anomalies. The abscissa describes regions with size progressively increasing from left to right, starting from the equatorial eastern Pacific. To show the significance of these regression relations, we treat the regression slopes as statistical variables. They follow normal distributions, and their variances can be evaluated from the sample of 60-months of data. Since both the SST anomalies and the regression residuals of the cloud forcings are autocorrelated, the effective numbers of the degrees of freedom in the estimation of

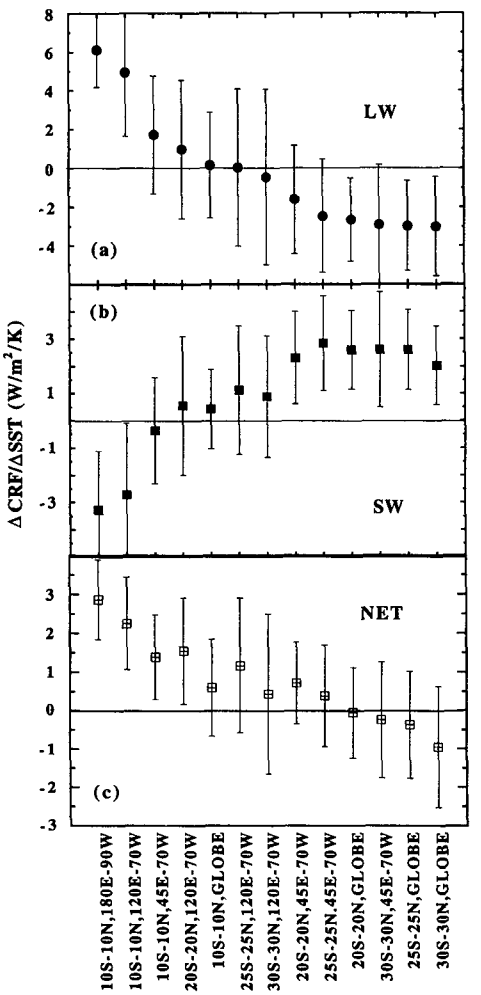

FIG. 7. Regression ratios of the (a) LW CRF, (b) SW CRF, and (c) Net CRF against SSTs for different regions as evaluated in Fig. 6. Error bars represent 95% confidence level of the regression slopes in (a) and (b) and 80% confidence level in (c).

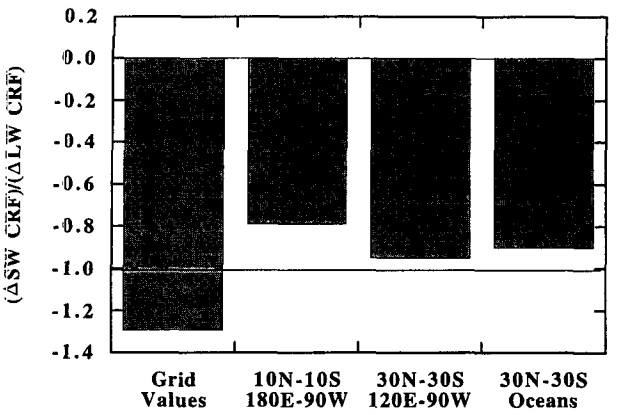

FIG. 8. Regression ratios of the SW CRFs against the LW CRFs using all monthly anomalies.

the variances of the regression slopes are substantially less than 60. The range in which the slopes should be, within a 95% confidence, is given in Figs. 7a and 7b as error bars for the LW and SW CRFs. Error bars in Fig. 7c represent the 80% confidence interval. These error bars also provide information on the probability for the regression slopes to exceed or fall below the indicated ranges. Although the uncertainties are large, due to large scatters such as those shown in Fig. 6, the analysis shows the signs of the regression slopes for LW CRF and SW CRF with large confidence. Note that ΔCRF/ΔSST changes sign as the size of the region changes. For the entirety of the Tropics (30°S–30°N, GLOBE), the LW ΔCRF cooling (LW CRF decreases with SST) and SW ΔCRF warming (SW CRF increases with SST) are well within the 95% confidence levels. The LW ΔCRF/ΔSST is about -3.0 W m^{-2} K^{-1}, the SW ΔCRF/ΔSST is about 2 W m^{-2} K^{-1}, and the net ΔCRF/ΔSST is about -1.0 W m^{-2} K^{-1}. We note that these rates are not the same as those in Fig. 4 taken from the 6-month averages of the data, where the time samples are too small to give a statistical significance analysis.

The regression ratios of the LW CRF and SW CRF are of opposite signs in most of the regions. Consistent with Fig. 4, the net ΔCRF/ΔSST follows that of the longwave at the two ends of the size spectrum—it is negative for the tropical oceans as a whole, but it is statistically insignificant. More observational data are needed to assess the confidence level. It should be pointed that this small net effect is also consistent with the regression relationship between the LW and SW CRFs. Figure 8 shows that when dealing with gridpoint values (only in some specific regions), the variation of the SW CRF is larger than that of the LW CRF. For area-averaged CRFs, variations of SW CRF are slightly smaller than those of the LW CRF, leaving the net variation of CRF to follow that of the LW CRF. This phenomenon is presumably due to large variability of high clouds that have stronger impacts on longwave radiation than on shortwave radiation. However, further study is needed (Kiehl 1994).

The data used above include all monthly data for describing interannual variability. To examine whether there is seasonal dependence in the relationship, we further categorize the data into different seasons and regress the interannual variability of CRFs for each season against the interannual variability of SSTs. Figure 9 shows that the signs of the longwave and shortwave CRF–SST relationships are consistent in all four seasons. The relationships for the net CRF have an exception in the September–November season, when there is an insignificant magnitude; in all other seasons, they follow the signs of the LW CRF.

c. *Discussion about the cause of the sign reversal*

The above discussion suggests the importance of including the entire Walker and Hadley circulations for the interpretation of cloud–climate interactions. In Figs. 10a and 10b we show the geographical distribution of changes in LW and SW CRFs from the period of January 1985–June 1986 to that of January 1987–June 1988. They should be discussed in conjunction with Fig. 1, which shows SST variations between the two periods. In response to the broad SST increases, only in the area with the largest positive SST anomalies does the LW CRF increase and SW CRF decrease, in agreement with previous regional studies. Yet, opposite compensatory changes occur in a much broader region, even when SST anomalies are still positive, such as in the Indian Ocean and the Atlantic. Figure 10c shows the variation of total cloud amount between the two periods in the ISCCP data. Variations of the CRFs are

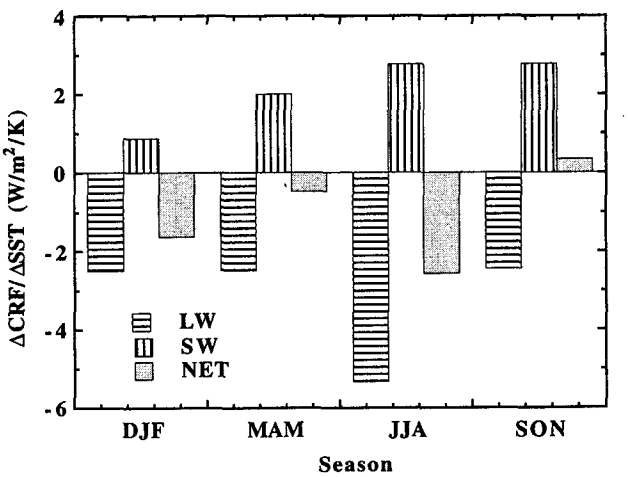

FIG. 9. Relationships between CRFs and SSTs in different seasons for the entire tropical oceans.

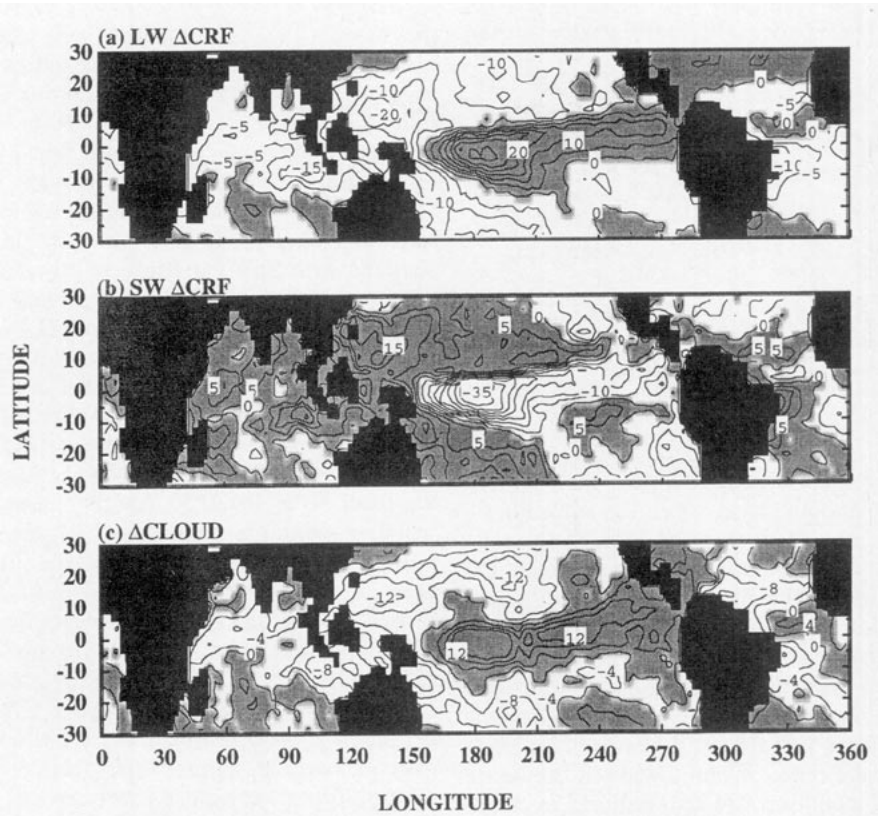

FIG. 10. Changes of (a) LW CRF, (b) SW CRF, and (c) total cloud amount from the period of January 1985–June 1986 to the period of January 1987–June 1988. Gray represents positive. White represents negative. Contour intervals in (a) and (b) are 5 W m^{-2}, and the interval in (c) is 4%.

consistent with the variations of cloud amount to the first order.

Studies that used the tropical Pacific to examine the SST–CRF relationship reported that the averaged cloud forcing is not related to the averaged SST in a significant way (Fu et al. 1992; Hartmann and Michelesen 1993; Chou 1994). This is due to the compensatory variations of clouds between the western tropical Pacific and the equatorial central and eastern Pacific. The impact of the descending branch of the Hadley circulation on the cloud variation is evident in Fig. 10 in the western and central Pacific. But CRF and SST also change in the Indian Ocean and the Atlantic, and they are large enough to make a significant contribution to the sign of the CRF–SST relationship for the whole of the Tropics.

Meehl (1987) and Godfrey (1994) reported that SSTs in the Indian Ocean warm up in a composite El Niño event, and the magnitude could be as much as 0.4 K. This is consistent with the present study for the 1987 El Niño. Villwock and Latif (1994) reported that SST variations in the central and eastern tropical Pacific are typically followed by SST anomalies of the same sign in the Indian Ocean. The reason for this warming is not clear. Hirst and Godfrey (1993) suggested that the open passage at the southern tip of the Indonesia makes warm ocean currents cross the Indian Ocean, and these warm the SSTs there during an El Niño event. To the contrary, Villwock and Latif (1994) argued that the surface wind forced by SST anomalies in the equatorial Pacific is the primary cause of the SST warming in the Indian Ocean. SST anomalies may even be a result of the cloud variations. All these studies reported that during an El Niño year, surface insolation is increased over the Indian Ocean. Villwock and Latif (1994) estimated this increase to be as large as 20 W m^{-2}. Thus, it is likely that the phenomena we reported here with the 1987 El Niño also exists in other El Niño events.

It is tempting to attribute the decrease of clouds over the Indian Ocean during a warm year to the impact of the descending branch of Walker circulation, which is associated with the enhanced upward branch in the central and equatorial Pacific. However, it is known that the Walker circulation to the west of the upward branch does not extend as far as that to its east, and the pattern does not resemble those of the Rossby gravity wave structures (Gill 1980). Another possibility is that the descending branch of the Walker circulation to the east

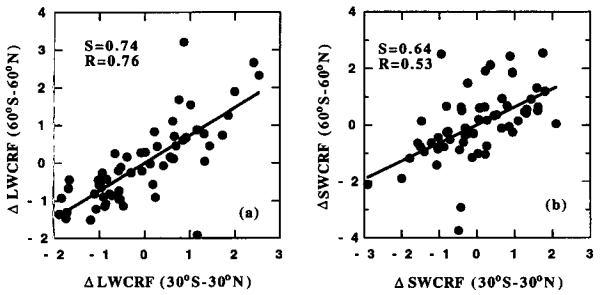

FIG. 11. CRF variations averaged from 60°N to 60°S versus those averaged over oceans from 30°N to 30°S using all monthly anomalies: (a) longwave and (b) shortwave.

of the ascending branch extends to pass through the Atlantic and to the Indian Ocean. Yet, the variation of the LW CRF does not show signs of increasing magnitude toward the west in the Indian Ocean. The anomaly of vertical motion from the ECMWF analysis actually shows ascending motion over the Indian Ocean instead of a descending motion.

There are other possible explanations for the decrease in clouds over the Indian Ocean. One is that clouds over the Indian Ocean could be advected from the western tropical Pacific. When clouds in the western Pacific are reduced, they are also reduced over the Indian Ocean, regardless of the fact that local SSTs are increased. The second possible explanation would be that clouds are related to the surface wind because wind speed changes over the Indian Ocean during an El Niño event. The third is that the change in clouds is related to the Indian monsoon. This third cause may be more plausible than the others, since it is well known that monsoon activity is much weaker during an El Niño year than it is in a La Niña year. Clouds associated with the monsoon system are therefore reduced, even when the local SSTs are warmer. Thus, regional features of cloud variations associated with the Asia monsoon may have strongly affected the sign of cloud variations in the whole of the Tropics. This links to the possible impact of other factors that may affect the Indian monsoon, such as snow and land surface boundary conditions over the Himalayas.

No matter what the causes are, this phenomenon of warm SSTs and fewer clouds in the Indian Ocean and the Atlantic offers a challenge to the general circulation models in terms of correctly simulating the CRF–SST relationship over all of the Tropics.

4. Discussion

Here, we bring up several issues that are pertinent to the interpretation of the present results. The first is the selection of the area used in the averaging. As discussed in the introduction, the best choice is to use the whole globe. But this would compromise the signal of the cloud–SST relationships, not only because the global mean surface temperature varies little from year to year, but also because natural variability at higher latitudes is large. The choice of 30°N to 30°S is somehow arbitrary. One may argue that 40°N to 40°S or 50°N to 50°S would also be relevant for this type of study. Indeed, if there are large compensatory variations of clouds from the middle and high latitudes associated with SST variations at low latitudes, it is necessary to include these regions as well. Figure 11 plots the CRF variations averaged from 60°N to 60°S against those averaged over oceans from 30°N to 30°S. It is seen that the trends are the same, and so there are no large compensatory changes in clouds from the middle and higher latitudes. The same is true when we used latitude belts other than 60°N to 60°S. For this reason, we used 30°N to 30°S. Another relevant question is whether including land areas between 30°N and 30°S will change our results. Land area occupies a small percentage of the surface from 30°N to 30°S. Figure 12 shows the averaged CRFs over tropical oceans versus CRFs averaged over tropical oceans and land combined. The two are very well correlated. We have also examined the relationship between CRFs and air temperatures at 1000 mb from the ECMWF analysis, both averaged over all surface types from 30°N to 30°S. The relationship is very close to what we obtained by using data over tropical oceans alone.

The second issue concerns the accuracy of the data. The signatures we studied here are about 2 to 3 W m^{-2} K^{-1}. This is significant if compared with the ratio of the CO_2 forcing to its directly induced temperature change (4 W m^{-2} vs 1.2 K). But measurement errors of radiation may exceed 5 W m^{-2}. We note that the variables we used are anomalies instead of absolute fluxes. Systematic measurement errors in both the radiation and SSTs are eliminated by the use of the anomalies. Furthermore, we used area-averaged anomalies over a large domain, which is likely to minimize random errors. The coherent patterns of the changes in the LW and SW CRFs, as shown in Fig. 10, suggest that the changes are controlled by

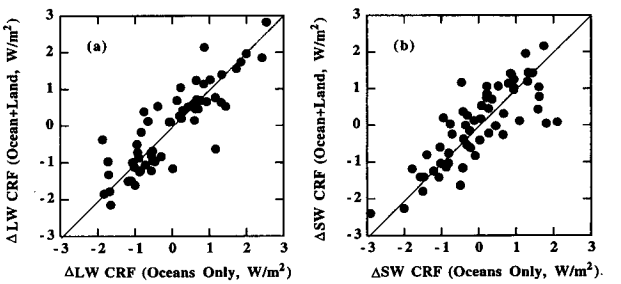

FIG. 12. CRF variations averaged over land and oceans combined from 30°N to 30°S versus those averaged over oceans from 30°N to 30°S using all monthly anomalies: (a) longwave and (b) shortwave.

physical processes rather than by random measurement errors. Because we used CRFs, there is another potential error source that comes from the clear-sky fluxes processed through ERBE. As illustrated in Fig. 5, since we can just use the outgoing longwave radiation at the TOA to reach the same conclusion, we believe the reported relationship is real.

The third issue concerns the applicability of the current finding of cloud–climate interaction to other climate changes. We do not expect the CRF–SST relationship reported here to hold for the seasonal cycle of the tropical climate because there is also a strong seasonal component in the lateral boundaries exerted by middle-latitude circulations. In the case of other El Niño events, we have pointed out that SSTs in the Indian Ocean warm up, and the surface insolation seems to increase during other El Niño years. An open question is whether these features in the Indian Ocean also produce the same CRF–SST relationship for the whole of the Tropics. As to the global warming scenario, the applicability of our results is limited by two factors. The first is the difference in the form of climate forcing. The forcing employed in this study is the internal oscillation of the coupled tropical ocean–atmosphere system with El Niño as a main feature of the SST variation, while the forcing in a CO_2 climate change is relatively uniform to the surface and in the atmosphere. It is almost certain that cloud–climate feedback is dependent on the type of climate forcing. The second factor is the role of middle- and high-latitude circulation in determining the behaviors of cloud variations. The present study is restricted to the Tropics. In a CO_2 climate change, circulation changes in middle and high latitudes are expected to affect not only the CRF there but also the tropical circulations.

5. Conclusions

In summary, we have shown that variation of clouds causes reduction of longwave trapping when the SST is warmer in all of the Tropics during the period of 1985–1989. The rate is about -3 W m^{-2} K^{-1}. This loss of radiative energy is partly compensated for by less cloud reflection of solar radiation to space, with a rate of 2 W m^{-2} K^{-1} to the system's energy balance, as SST warming occurs associated with an El Niño event.

This phenomenon appears only when the region considered is extended beyond the tropical Pacific. Over the Indian Ocean and the Atlantic, warm SST anomalies are found to be associated with less cloud forcing, and these features affect the sign of the cloud impact averaged over the Tropics as a whole. It is speculated that the change of clouds over the Indian Ocean may be related to variations of monsoon activities.

The clouds–SST relationships reported here for different regions provide a scenario for testing and validating climate models dealing with cloud–climate interactions. They also point out a more difficult challenge to the study of the cloud feedback problem; that is, process studies of cloud–radiation interaction at individual locations need to include regions that are dynamically connected, which encompasses virtually the entire globe.

Acknowledgments. We thank Drs. V. Ramanathan, Marvin Geller, and Duane Waliser for their helpful comments on an early version of our manuscript. We also thank Mr. Xiaodan Lu for assisting us in processing the data. Comments from the two anonymous reviewers and Dr. James Coakley have improved several aspects of the manuscript, particularly the confidence interval analysis in Fig. 7. This research is supported by NASA under Grant NAG3517 and by the Department of Energy under Grant DEFG0285ER60314 to the State University of New York at Stony Brook.

REFERENCES

Arking, A., and D. Ziskin, 1994: Relationship between clouds and sea surface temperatures in the western tropical Pacific. *J. Climate,* **7,** 988–1000.

Barkstrom, B. R., and G. L. Smith, 1986: The Earth Radiation Budget Experiment: Science and implementation. *Rev. Geophys.,* **24,** 379–390.

Cess, R. D., and Coauthors, 1990: Intercomparison and interpretation of climate feedback processes in 19 atmospheric general circulation models. *J. Geophys. Res.,* **95,** 16 601–16 615.

——, and G. L. Potter, W. L. Gates, J. J. Morcrette, and L. Corsetti, 1992: Comparison of general circulation models to Earth Radiation Budget Experiment data: Computation of clear-sky fluxes. *J. Geophys. Res.,* **97,** 20 421–20 426.

——, and Coauthors, 1996: Cloud feedback in atmospheric general circulation models: An update. *J. Geophys. Res.,* in press.

Chou, M. D., 1994: Coolness in the tropical Pacific during an El Niño episode. *J. Climate,* **7,** 1684–1692.

Fu, R., A. D. Del Genio, W. B. Rossow, and W. T. Liu, 1992: Cirrus-cloud thermostat for tropical sea surface temperatures tested using satellite data. *Nature,* **358,** 394–397.

Gill, A. E., 1980: Some simple solutions for heat-induced tropical circulation. *Quart. J. Roy. Meteor. Soc.,* **106,** 447–462.

Godfrey, J. S., 1994: A literature review of SST anomalies in the Indian Ocean: Their effects on the atmosphere and their causes. *Proc. Int. Conf. on Monsoon Variability and Prediction,* Trieste, Italy, World Climate Research Programme, 524–529.

Harrison, E. F., P. Minnis, B. R. Barkstrom, V. Ramanathan, R. D. Cess, and G. G. Gibson, 1990: Seasonal variation of cloud radiative forcing derived from the Earth Radiation Budget Experiment. *J. Geophys. Res.,* **95,** 18 687–18 703.

Hartmann, D. L., and M. Michelsen, 1993: Large-scale effects on the regulation of tropical sea surface temperature. *J. Climate,* **6,** 2049–2062.

Hirst, A. C., and J. S. Godfrey, 1993: The role of the Indonesia Throughflow in a global ocean GCM. *J. Phys. Oceanogr.,* **23,** 1057–1086.

IPCC, 1990: *Climate Change, the IPCC Scientific Assessment.* Cambridge University Press.

Kiehl, J. T., 1994: On the observed near cancellation between longwave and shortwave cloud forcing in tropical regions. *J. Climate,* **7,** 559–565.

Meehl, G. A., 1987: The annual cycle and interannual variability in the tropical Pacific and Indian Ocean regions. *Mon. Wea. Rev.,* **115,** 1057–1086.

Mitchell, J. F. B., C. A. Senior, and W. J. Ingram, 1989: CO_2 and climate: A missing feedback? *Nature,* **341,** 132–134,

Philander, S. G., 1990: *El Nino, La Nina, and the Southern Oscillation.* Academic Press, 293 pp.

Potter, G. L., J. M. Slingo, and J. J. Morcrette, 1992: A modelling perspective on cloud-radiative forcing. *J. Geophys. Res.,* **97,** 20 507–20 518.

Ramanathan, V., and W. Collins, 1991: Thermodynamic regulation of ocean warming by cirrus clouds deduced from observations of the 1987 El Nino. *Nature,* **351,** 27–32.

——, R. D. Cess, E. F. Harrison, P. Minnis, B. R. Barkstrom, E. Ahmad, and D. Hartmann, 1989: Cloud-radiative forcing and climate: Results from the Earth Radiation Budget Experiment. *Science,* **243,** 57–63.

Randall, D. A., and Coauthors, 1992: Intercomparison and interpretation of surface energy fluxes in atmospheric general circulation models. *J. Geophys. Res.,* **97,** 3711–3725.

Reynolds, R. W., 1988: A real-time global sea surface temperature analysis. *J. Climate,* **1,** 75–86.

Trenberth, K. E., and D. J. Shea, 1987: On the evolution of the southern oscillation. *Mon. Wea. Rev.,* **115,** 3078–3096.

Villwock, A., and M. Latif, 1994: Indian Ocean response to ENSO. *Proc. Int. Conf. on Monsoon Variability and Prediction,* Trieste, Italy, World Climate Research Programme, 530–537.

Wetherald, R. T., and S. Manabe, 1988: Cloud feedback processes in general circulation models. *J. Atmos. Sci.,* **45,** 1397–1415.

Zhang, M. H., R. D. Cess, T. Y. Kwon, and M. H. Chen, 1994: Approaches of comparison for clear-sky radiative-fluxes from general circulation models with Earth Radiation Budget Experiment data. *J. Geophys. Res.,* **99,** 5515–5523.